A confocal microscopy image analysis method to measure adhesion and internalization of *Pseudomonas aeruginosa* multicellular structures into epithelial cells

Paola Lepanto [a], Federico Lecumberry [b,1], Jéssica Rossello [a,1], Arlinet Kierbel [a,c,*]

[a] Institut Pasteur de Montevideo, Montevideo 11400, Uruguay
[b] Instituto de Ingeniería Eléctrica, Facultad de Ingeniería, Universidad de la República, Julio Herrera y Reissig 565, Montevideo 11300, Uruguay
[c] Instituto de Investigaciones Biotecnológicas Dr. Rodolfo A. Ugalde (IIB-INTECH), Universidad Nacional de San Martín, Consejo Nacional de Investigaciones Científicas y Técnicas (UNSAM-CONICET), San Martín, Buenos Aires, Argentina

ARTICLE INFO

ABSTRACT

Formation of multicellular structures such as biofilms is an important feature in the physiopathology of many disease-causing bacteria. We recently reported that *Pseudomonas aeruginosa* adheres to epithelial cells rapidly forming early biofilm-like aggregates, which can then be internalized into cells. Conventional methods to measure adhesion/internalization, such as dilution plating for total cell-associated or antibiotic protected bacteria, do not distinguish between single and aggregated bacteria. We report a procedure that combining double bacteria labeling, confocal microscopy and image analysis allows identification and quantification of the number of adhered and internalized bacteria distinguishing between single and aggregated bacterial cells. A plugin for Fiji to automatically perform these procedures has been generated.

© 2013 Published by Elsevier Ltd.

1. Introduction

Although a unicellular view of bacteria has been predominant in the past, it is now evident that bacteria communicate with and physically contact other bacteria, developing coordinated behavior and the formation of complex multicellular structures. Such microbial behaviors are often critical in the setting of infections. Growing evidence shows that biofilms, defined as surface-associated bacterial communities encased in an extracellular matrix, are not just prevalent in natural but also in pathogenic ecosystems [1].

Enteropathogenic *Escherichia coli*, *Bortadella pertussis*, *Pseudomonas aeruginosa*, *Streptococcus pyogenes* and *Neisseria gonorrhoeae* are example pathogenic bacteria that have been shown to interact with host cells forming multicellular structures. Formation of such structures is often correlated with virulence and it is observed both *in vivo and in vitro* [2 7].

P. aeruginosa growth as biofilms in lungs of cystic fibrosis (CF) patients [8] is a key factor leading to antibiotic resistance and fatality in these chronic airway infections [9,10]. We were recently able to monitor the early stages of apical colonization of polarized epithelial cells leading to the formation of *P. aeruginosa* early biofilm-like aggregates in real-time. Over 90% of bacteria that become associated with the epithelial surface were found in such multicellular structures [11].

Upon attachment, some pathogenic bacteria get internalized into non-phagocytic cells. This behavior often constitutes an important survival strategy [12 14]. Internalization of *P. aeruginosa* into epithelial cells has been shown to occur both *in vivo* as *in vitro* [15 20], although its role in the infection process is not clearly defined yet. Noteworthy, previous work including our, showed the presence of *P. aeruginosa* intracellular biofilm like-aggregates [11,21].

Bacterial adhesion and internalization are typically measured by plating serial dilutions and counting colony forming units to determine total cell-associated or antibiotic-protected bacteria respectively [22,23]. These methodologies, however, are unable to distinguish between single and aggregated bacteria. As noted above, quantitative determination of the different bacterial populations that associate with the host cells is relevant to understanding pathogenic bacteria-host cells interaction. Quantitation of single and aggregated

---

bacteria by manual counting using fluorescence microscopy images is possible, but it is time-consuming and laborious. Here we report a procedure that utilizes double bacteria staining, confocal microscopy and image analysis to determine the number of surface-attached and internalized bacteria. Moreover, the method also determines whether the bacteria are associated with the cell individually or in multicellular structures. A plugin for Fiji that automatically performs image analysis procedures is also presented.

2. Materials and methods

2.1. Reagents

Anti-*P. aeruginosa* antibody was obtained from AbCam (ab68538, dilution 1/100) (Cambridge MA, USA). Alexa-647 conjugated phalloidin, Alexa-647 conjugated anti-rabbit and TRITC conjugated anti-rabbit were acquired from Life Technologies. LY294002 was purchased from Sigma—Aldrich (St. Louis, MO, USA) and used at a concentration of 50 µM.

2.2. Cell culture and bacterial infection

Wild-type MDCK (clone II) cells, MDCK cells stably expressing the pleckstrin homology (PH) domain of Akt fused to Green Fluorescent Protein (GFP-PH-Akt) [24] or E-Cadherin-Red Fluorescent Protein (E-Cadherin-RFP, kindly provided by W. James Nelson (Stanford University, Stanford, California)) were cultured in minimal essential medium (MEM) containing 5% fetal bovine serum at 37 °C in a 5% CO_2 atmosphere. Cells were seeded (0.8×10^6 cells per well) on trans-wells (0.4 mm pore size, Corning Fisher, NY) and used for experiments after incubation for 24 h.

P. aeruginosa strain K was routinely grown in Luria—Bertani broth shaking overnight at 37 °C. Fluorescence microscopy studies were done with *P. aeruginosa* carrying plasmids expressing either m-Cherry [25] or GFP [26]. Stationary phase bacteria were co-cultivated with MDCK cells monolayers using a multiplicity of infection of 60 for 30 min or 2 h as indicated. For LY294002 treatment cells were pre-incubated for 1 h with MEM containing the drug and bacterial inoculations were done in the presence of the drug.

2.3. Immunofluorescence sample preparation and laser scanning confocal microscopy (LSCM)

Infected MDCK monolayers were washed three times with phosphate-buffered saline (PBS) and fixed in 4% paraformaldehyde for 30 min at room temperature. Samples were blocked with fish skin gelatin 0.7% in PBS and incubated over-night at 4 °C with primary antibody and for 1 h at room temperature with secondary antibody. Cell permeabilization was carried out, when indicated, by incubation in 0.1% TritonX100 in PBS for 30 min at room temperature. Samples were examined with a confocal microscope (Leica TCS-SP5) using a HCX PL APO 63x/NA1.4—0.60 CS oil objective. Confocal stacks were acquired with z-spacing of 0.2 µm from 10 randomly selected fields/condition. Settings were adjusted so that the range of fluorescence intensity of a given sample matched the range of pixel values available (i.e. so that, pixel values of cero and saturation were avoided). 3D reconstructions were made using 3D Viewer plugin for ImageJ [27].

3. Results and discussion

3.1. Identification and quantitation of individual and aggregated cell-associated bacteria

Polarized MDCK cells stably transfected with PH-AKT-GFP (a phosphatidylinositol 3,4,5-trisphosphate probe that localizes at the basolateral membrane) were infected for 30 min with *P. aeruginosa* expressing mCherry (PA-mCh), fixed and imaged by LSCM. The stack of images from the bacterial channel (mCherry) was analyzed using the 3D-Object Counter plugin for ImageJ [11]. This plugin identifies and enumerates the objects in the stack with a user-defined threshold for voxel intensity value. This limit intensity value separates voxels into distinct populations: background voxels (intensities below the selected value) and objects voxels. Contiguous object voxels are tagged together and considered part of the same particle. The plugin generates a binary mask showing the particles and provides a list of the particles with their respective volumes (Fig. 1B, C). The value of the voxel intensity threshold was set manually by visual inspection of the images (Image J: *Image ▷ Adjust ▷ Threshold*). This threshold was defined so that all bacteria in the stack were included and bacteria appearing physically together in 3D reconstructions were considered to be part of the same particle. The size of one bacterium was in average, with our acquisition settings, 206 ± 96 voxels (mean ± SD of 558 individual bacteria from 9 independent experiments). Thus, to avoid particles formed from background fluorescence to be included in the list, the minimal size of particles to be considered was set in ~100 voxels. As observed, single bacteria volume was somewhat variable. This is probably due to variations in the level of fluorescent protein expression. The estimate of the number of bacteria in each particle was made considering the volume of the particle divided by the mean volume of single bacteria in the field being analyzed.

We next compared this method with manual counting of bacteria in 3D reconstructions. To do this, a total of 261 particles were selected from 4 different experiments and the number of bacteria per particle was estimated using both methods. As shown in Fig. 1D, use of the image analysis method resulted in values very similar to those obtained by manual counting.

3.2. Determination of bacteria cellular location

We recently showed that both, *P. aeruginosa* aggregates formed on the surface as well as single attached bacteria are capable of being rapidly internalized into epithelial cells [11]. In that study, we determined whether bacteria were extracellular or intracellular by visual inspection: the location of each particle was assigned based on appearance in composite images. These composite images included the bacterial channel, the mask of the particles and a channel corresponding to the epithelial cell boundaries (i.e. by phalloidin staining). Such methods are labor intensive and time consuming. The analysis has since been streamlined and automated using a second bacterial stain and by including image analysis as outlined below.

Polarized MDCK cells were infected for 2 h with PA-GFP, fixed and immunostained with an anti-PA antibody followed by TRITC conjugated secondary antibody. Epithelial cells were stained for actin using Alexa-647 conjugated phalloidin. When samples were not permeabilized, the antibody was unable to reach intracellular bacteria, and therefore, only extracellular bacteria were labeled (Fig. 2A, upper panel). In controls with permeabilized cells, anti-PA antibody also recognized intracellular bacteria (Fig. 2A, lower panel).

To identify intracellular and extracellular bacteria, images from not permeabilized samples, were analyzed in three steps: 1) a binary mask of the antibody channel highlighting extracellular bacteria was generated. (The threshold value was set manually by visual inspection so that all the bacteria stained by the antibody were completely included into the mask). 2) The mask was subtracted from the bacterial channel, giving intracellular bacteria as a result 3) The logical AND operation was performed between the
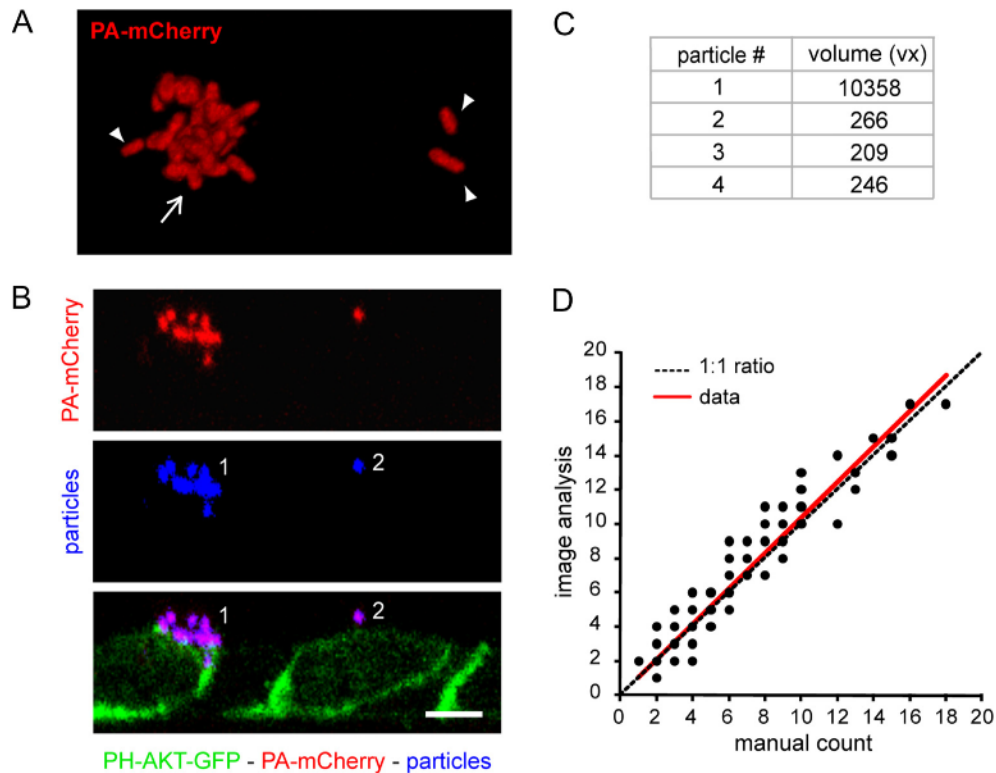
Fig. 1. Identification of aggregated and single cell-associated bacteria. Counting bacteria by confocal microscopy and image analysis. Example of the analysis procedure performed on a field portion containing one aggregate and three single bacteria A. 3D reconstructions showing the aggregate (arrow) and the single bacteria (arrowheads). B. Orthogonal sections showing the aggregate and one bacterium. Upper panel: bacterial channel. Middle panel: particles detected and numbered by the 3D Object Counter plugin. Lower panel: merged image. (scale bar: 5 μm) C. List of the particles and their corresponding volumes (in voxels - vx). Particles 2, 3 and 4 correspond to single bacteria (mean single bacterial volume − 240 voxels). Particle 1 corresponds to the aggregate and consists of roughly 43 bacteria (10358/240). D. Comparison of image analysis and manual counting methods. A total of 261 particles were analyzed (some points of the curve are overlapping). Data presented in a linear relationship ($y − 1.0402x − 0.0245$, $r − 0.92$).

mask and the bacterial channel, giving extracellular bacteria as a result. (AND is a logical operator that takes two images as input and produces as output a third image whose TRUE (i.e. non-zero) pixels are those that are TRUE in both input images). To illustrate the process, images of MDCK cells expressing the basolateral marker E-cadherin-RFP infected with PA-GFP and stained with anti-*P. aeruginosa* antibody are presented (in this case the secondary antibody was conjugated to Alexa-647). Fig. 2B displays an image that shows several bacteria associated to the epithelial cell monolayer. Some bacteria are aggregated while some are individually associated. And some bacteria are extracellular while some are intracellular (See also Supplementary Video S1). Internalized bacteria are green while extracellular are light blue. Fig. 2C illustrates (for the same image) the generation of the antibody channel mask and the operations to obtain both the intracellular and the extracellular signal.

Supplementary data related to this article can be found online at http://dx.doi.org/10.1016/j.mcp.2013.10.001.

Aggregates containing both, extra and intracellular bacteria are sometimes found as we previously reported [11]. These situations probably represent the partial internalization of surface formed-aggregates. In such cases, the host cell membrane would be between the intra and the extracellular part of the aggregate. However, the resolution of the system is not enough to detect the distance imposed by the presence of the membrane and both parts of the aggregate are perceived as one particle. These aggregates are classified as intermediates (see Section 3.3).

Determination of bacterial position by image analysis of double stained bacterial samples was compared with former visual inspection method rendering almost identical results (not shown).

3.3. Automated image analysis software

The procedures presented in Sections 3.1 and 3.2 were implemented as a plugin for Fiji. This software is available for download from https://www.pasteur.edu.uy/bcm/plugin. Two stacks of images are used as input. One stack corresponds to the bacterial channel and the other stack corresponds to the antibody channel highlighting extracellular bacteria. The antibody channel is used to generate an extracellular mask. This mask is subtracted from the bacterial channel to generate a new stack with only the intracellular signal. The logical AND operation is then performed between the same mask and the bacterial channel to generate a new stack with only the extracellular signal. Objects in the bacterial channel, the intracellular and the extracellular stacks are identified and counted using the Fiji 3D Object Counter plugin. Three particle lists are generated 1) total particles, 2) intracellular particles and 3) extracellular particles. These lists contain the particle ID, their volume in voxels and the 3D coordinates of their centroids. Then the algorithm computes the distances between the centroids of all the particles in list 1, with the centroids of all the particles in list 2 and 3. When a centroid from list 1 coincides (or the distance is less than a pixel) with a centroid from list 2 or 3, the particle cellular location is tagged as INTRACELLULAR or EXTRACELLULAR respectively. Particles that do not fit in this classification are tagged as INTERMEDIATE. The plugin gives an output list containing a) particles ID, b) particles volume (in voxels) c) particle cellular location (i.e. extracellular, intermediate or intracellular) and d) an image with the objects identified by the 3D object counter (Fig. 2D and E in our example).
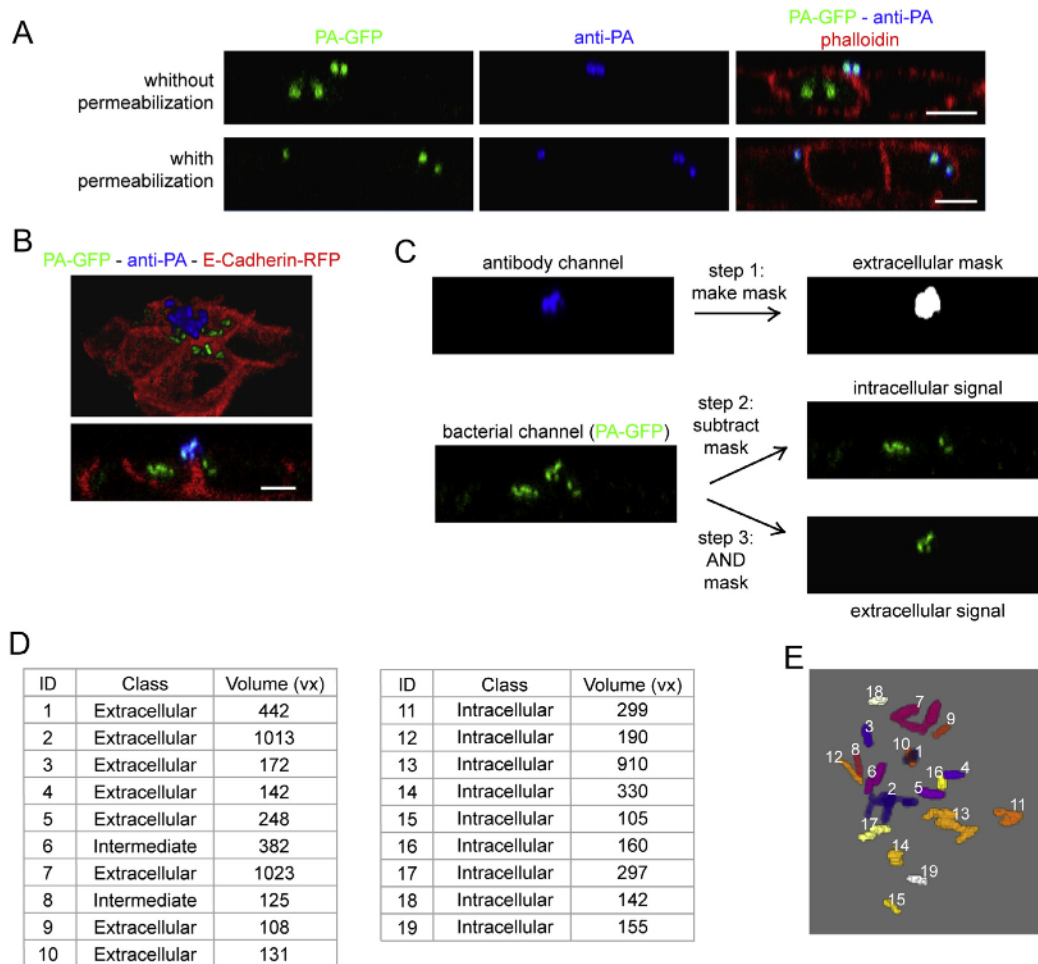
Fig. 2. Extracellular and intracellular bacteria identified by immunostaining and image analysis. A. Orthogonal sections of confocal microscopy stacks from samples stained with anti-PA antibody using non-permeabilized or permeabilized cells. B. 3D reconstruction and orthogonal section of the stack analyzed in C–E. C. Work flow of the image analysis procedure to identify intracellular and extracellular bacteria. Images acquired from non-permeabilized samples are processed in the following way: (step 1) anti-PA channel is used to generate a mask (threshold used − 40), (step 2) this mask is subtracted from PA-GFP channel (Image Calculator/Subtract) and (step 3) logical AND operation between the mask and the PA-GFP channel (Image Calculator/AND). Finally, 3D object detection is carried out in the original PA-GFP channel and in the resulting intracellular and extracellular stacks (threshold used: 70, min: 100). Scale bars: 5 µm. D. Output list given by the software. E. 3D rendering (3D Viewer) of the output image given by the software showing the particles with their ID.

Note that in the presented example a single bacterial cell is classified as intermediate (ID 8). This might represent a technical artifact produced by inaccessibility of the antibody to zones of the bacterium in close contact with the host cell membrane. Cases like this were found very infrequently.

The number of bacteria per particle can be estimated dividing the volume of each particle by the volume corresponding to a single bacterial cell. This value will depend on the particular microorganism the user is working with as well as on the sample and the acquisition settings. Single bacteria are easily identified in the merged image of the bacterial channel and the objects map given by the 3D Object Counter plugin.

3.4. Effect of LY294002 on P. aeruginosa internalization measured by double labeling/image analysis method

We previously showed, by counting colony forming units in standard antibiotic protection assays, that treatment with 50 µM LY294002, an inhibitor of Phosphoinositide 3-kinase, impairs *P. aeruginosa* entry into polarized MDCK cells [28]. The effect of LY294002 on *P. aeruginosa* internalization was assayed to further validate our method. When assayed using the double labeling/image analysis method presented here, our previous result was reproduced. Furthermore, new method showed that LY294002 inhibition affects both, entry of single and aggregated bacteria (Fig 3).

3.5. Conclusions

We have developed an automated and quantitative methodology to determine number of attached and internalized bacteria, distinguishing between single and aggregated one. Association of bacteria with host cells as multicellular aggregates is emerging as a common feature in pathogenic bacteria-host cell interaction. Surface attachment and microcolony formation are also early key steps in biofilm development. Bacterial internalization may represent either a bacterial strategy for survival inside the host cells or a host cell defense mechanism. A better understanding of these processes as well as the screening of potentially inhibitory drugs clearly depend on the development of methods that quantitatively determine bacterial aggregation state and subcellular localization.
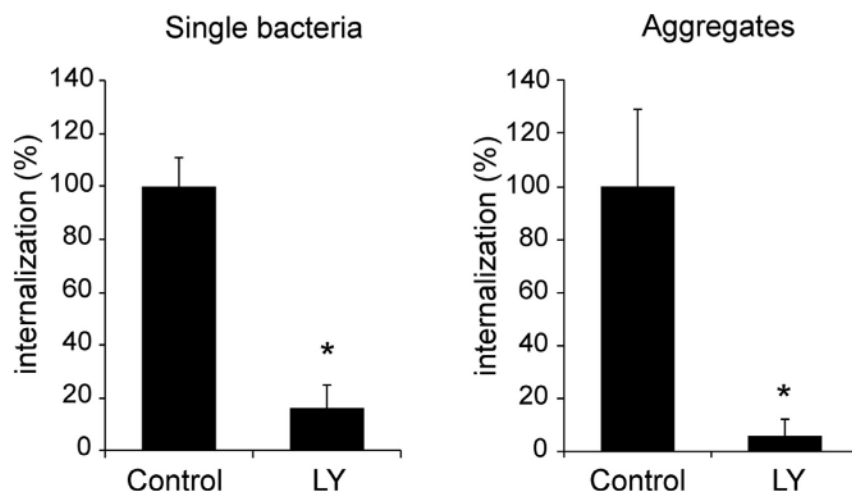
Single bacteria / Aggregates

Fig. 3. Effect of LY294002 on internalization of single and aggregated *P. aeruginosa* GFP-PH-Akt MDCK cells were treated with 50 μM LY294002 (LY) or vehicle (Control) and infected with m-Cherry *P. aeruginosa* for 2 h. Samples were fixed and imaged as described in section 1 and analyzed as described through sections 1 and 2. Graphs show the percentage of internalized individual bacteria or aggregates relative to cell associated individual bacteria or cell associated aggregates respectively. About 30 fields per condition from independent experiments were analyzed. Each field contained approximately 200 MDCK cells and about 85 associated bacteria. Data are represented as mean +/− standard deviation. Data was transformed using rank transformation [29] and compared using a mixed model nested ANOVA [30]. (*) $p < 0.05$.

References

[1] Costerton JW, Lewandowski Z, Caldwell DE, Korber DR, Lappin-Scott HM. Microbial biofilms. Annu Rev Microbiol 1995;49:711 45.
[2] Clausen CR, Christie DL. Chronic diarrhea in infants caused by adherent enteropathogenic *Escherichia coli*. J Pediatr 1982;100:358 61.
[3] Menozzi FD, Boucher PE, Riveau G, Gantiez C, Locht C. Surface-associated filamentous hemagglutinin induces autoagglutination of *Bordetella pertussis*. Infect Immun 1994;62:4261 9.
[4] Hassett DJ, Korfhagen TR, Irvin RT, Schurr MJ, Sauer K, Lau GW, et al. *Pseudomonas aeruginosa* biofilm infections in cystic fibrosis: insights into pathogenic processes and treatment strategies. Expert Opin Ther Targets 2010;14: 117 30.
[5] Frick IM, Morgelin M, Bjorck L. Virulent aggregates of *Streptococcus pyogenes* are generated by homophilic protein-protein interactions. Mol Microbiol 2000;37:1232 47.
[6] Winzer K, Falconer C, Garber NC, Diggle SP, Camara M, Williams P. The *Pseudomonas aeruginosa* lectins PA-IL and PA-IIL are controlled by quorum sensing and by RpoS. J Bacteriol 2000;182:6401 11.
[7] Park HS, Wolfgang M, van Putten JP, Dorward D, Hayes SF, Koomey M. Structural alterations in a type IV pilus subunit protein result in concurrent defects in multicellular behaviour and adherence to host tissue. Mol Microbiol 2001;42:293 307.
[8] Engel JN. Molecular pathogenesis of acute *Pseudomonas aeruginosa* infections. In: Hauser A, Rello J, editors. Severe infections caused by *Pseudomonas aeruginosa*. New York City: Kluwer Academic/Plenum Press; 2003. p. 201 30.
[9] Moreau-Marquis S, Stanton BA, O'Toole GA. *Pseudomonas aeruginosa* biofilm formation in the cystic fibrosis airway. Pulm Pharmacol Ther 2008;21:595 9.
[10] Hall-Stoodley L, Stoodley P. Evolving concepts in biofilm infections. Cell Microbiol 2009;11:1034 43.
[11] Lepanto P, Bryant D, Rossello J, Datta A, Mostov K, Kierbel A. *Pseudomonas aeruginosa* interacts with epithelial cells rapidly forming aggregates that are internalized by a Lyn-dependent mechanism. Cell Microbiol 2011;13: 1212 22.
[12] Patel JC, Galan JE. Manipulation of the host actin cytoskeleton by Salmonella all in the name of entry. Curr Opin Microbiol 2005;8:10 5.
[13] Anderson GG, Palermo JJ, Schilling JD, Roth R, Heuser J, Hultgren SJ. Intracellular bacterial biofilm-like pods in urinary tract infections. Science 2003;301:105 7.
[14] Pizarro-Cerda J, Kuhbacher A, Cossart P. Entry of *Listeria monocytogenes* in mammalian epithelial cells: an updated view. Cold Spring Harb Perspect Med 2012;2.
[15] Fleiszig SM, Vallas V, Jun C, Mok L, Balkovetz D, Roth MG, et al. Susceptibility of epithelial cells to *Pseudomonas aeruginosa* invasion and cytotoxicity is upregulated by hepatocyte growth factor. Infect Immun 1998;66:3443 6.
[16] Fleiszig SM, Zaidi TS, Pier GB. *Pseudomonas aeruginosa* invasion of and multiplication within corneal epithelial cells in vitro. Infect Immun 1995;63: 4072 7.
[17] Fleiszig SM, Zaidi TS, Fletcher EL, Preston MJ, Pier GB. *Pseudomonas aeruginosa* invades corneal epithelial cells during experimental infection. Infect Immun 1994;62:3485 93.
[18] Kierbel A, Gassama-Diagne A, Rocha C, Radoshevich L, Olson J, Mostov K, et al. *Pseudomonas aeruginosa* exploits a PIP3-dependent pathway to transform apical into basolateral membrane. J Cell Biol 2007;177:21 7.
[19] Kazmierczak B, Jou T-S, Mostov KM, Engel JN. *Pseudomonas aeruginosa* invasion of Madin Darby Canine Kidney (MDCK) cells is modulated by RhoAV14 expression. Mol Biol Cell 1998;9:386a.
[20] Grassmé H, Kirschnek S, Riethmueller J, Riehle Andrea, von Kürthy G, Lang F, et al. CD95/CD95 ligand interactions on epithelial cells in host defense to *Pseudomonas aeruginosa*. Science 2000;290:527 30.
[21] Garcia-Medina R, Dunne WM, Singh PK, Brody SL. *Pseudomonas aeruginosa* acquires biofilm-like properties within airway epithelial cells. Infect Immun 2005;73:8298 305.
[22] Tang PFV, Pucciarelli MG, Finlay BB. Methods to study bacterial invasion. J Microbiol Methods 1993;18:227 40.
[23] Kazmierczak BI, Jou T-S, Mostov K, Engel J. Rho-GTPase activity modulates *Pseudomonas aeruginosa* internalization by epithelial cells. Cell Microbiol 2001;3:85 98.
[24] Yu W, Datta A, Leroy P, O'Brien LE, Mak G, Jou TS, et al. Beta1-integrin orients epithelial polarity via Rac1 and laminin. Mol Biol Cell 2005;16:433 45.
[25] Mougous JD, Gifford CA, Ramsdell TL, Mekalanos JJ. Threonine phosphorylation post-translationally regulates protein secretion in *Pseudomonas aeruginosa*. Nat Cell Biol 2007;9:797 803.
[26] Bucior I, Mostov K, Engel JN. *Pseudomonas aeruginosa*-mediated damage requires distinct receptors at the apical and basolateral surfaces of the polarized epithelium. Infect Immun 2010;78:939 53.
[27] Schmid B, Schindelin J, Cardona A, Longair M, Heisenberg M. A high-level 3D visualization API for Java and ImageJ. BMC Bioinformatics 2010;11:274.
[28] Kierbel A, Gassama-Diagne A, Mostov K, Engel JN. The phosphoinositol-3-kinase-protein kinase B/Akt pathway is critical for *Pseudomonas aeruginosa* strain PAK internalization. Mol Biol Cell 2005;16:2577 85.
[29] Conover WJ, Iman RL. Analysis of covariance using the rank transformation. Biometrics 1982;38:715 24.
[30] Sokal R. In: Blume, editor. Biometry: the principles and practices of statistics in biological research 1979.